Aeroacoustics Conferences
30 May - 1 June, 2016, Lyon, France
22nd AIAA/CEAS Aeroacoustics Conference

Experimental Study of Quadcopter Acoustics and Performance at Static Thrust Conditions

Nanyaporn Intaratep[*], W. Nathan Alexander[†], William J. Devenport[‡]
Virginia Tech, Blacksburg, VA 24060

Sheryl M. Grace[§]
Boston University, Boston, MA 02215

and

Amanda Dropkin[**]
Aurora Flight Sciences, Cambridge, MA 02142

A quadcopter, DJI Phantom II, was tested in the Virginia Tech Anechoic Chamber to study its aeroacoustics performance. Noise and thrust measured by a single microphone and a load cell were acquired for 4 different rotor configurations, two plastic and two carbon fiber rotors. To study the effects of multi-rotor interaction, the quadcopter was also set to operate with 1, 2 and 4 rotors. Results of 4-rotor operation show that tones at the blade passing frequency, shaft rate and their harmonics dominate the quadcopter acoustic spectrum up to 6000 Hz without much deterioration. Also significant is a broadband hump present in the mid frequency range which increases over 10 dB above the broadband level at low frequencies. Motor noise is also noticeable in the mid frequency range. For a small-scaled rotor, thrust performance is greatly influenced by rotor configuration whereas its acoustic signature is only altered near mid and high frequencies resulting in 1-2 dB change in the OASPL for the same thrust setting. Having 1, 2 or 4 rotors operating does not affect the acoustic signature but a significant increase was found in broadband noise when switching from 2 non-adjacent rotors to 4 rotors.

I. Introduction

In recent years, small multi-rotor UAVs have been adapted from their recreational status to be utilized more in various civil applications, from film making[1] to remote photography for scientific studies[2,3]. The interest of global companies, like Google and Amazon, in advancing a point-to-point delivery service has also prompted huge interests in multi-rotor UAV development. Compared to fixed-wing unmanned air vehicles, the multi-rotor UAVs, commonly referred to as drones, have many advantages due to their vertical take-off and landing (VTOL) abilities, ease of deployment without launching platforms and hovering function at low altitude to enhance surveillance resolution. Nevertheless, those who operate such craft will attest to the fact that they are not quiet hindering their usage in applications where noise is restricted. Ditmer *et al.*[4] found that the use of drones to follow free-roaming black bears can cause additional stress to the animals as demonstrated by their increased heartrates. The heartrate also spikes up proportionally to the drones proximity and wind speed, two factors controlling the perceived noise levels. With non-military unmanned air vehicle business being on a global rise of 15-20% annually[5], community noise will become of prime concern as many of these drones would fly closer to residential areas.

Considering the size of these small drones (on the order of 0.5m in diameter or less), there is very little information available on performance and noise characteristics for rotors or propellers at this scale. Current multi-

[*] Research Assistant Professor, Department of Aerospace and Ocean Engineering, AIAA member
[†] Assistant Professor, Department of Aerospace and Ocean Engineering, AIAA member
[‡] Full Professor, Department of Aerospace and Ocean Engineering, AIAA Associate Fellow
[§] Associate Professor, Department of Mechanical Engineering, AIAA Associate Fellow
[**] Propulsion Research Engineer, AIAA Member

rotor vehicles generally employ small rotors where the chord Reynolds number is on the order of 10^5, treading the region of fully laminar to transitional boundary layers which yield different flow physics than large-scale helicopters or aircraft fans and propellers. There are many studies regarding small propeller aerodynamic performance for UAVs[6,7,8] but fewer were found on noise.

Wright[9] introduced a universal form of the acoustic spectrum for rotating machines, including features found in low speed rotors. One dominating noise source especially for low speed rotors is the laminar boundary layer vortex shedding noise which can be found as a second hump in the broadband part of the spectrum at high frequency. Another source of broadband noise in UAV propellers was identified as the presence of a laminar separation bubble which can thicken the boundary layer at the trailing edge, thus increasing trailing edge noise[10,11]. Boundary layer tripping was applied to reduce broadband noise by eliminating such separation bubble. Gur & Rosen[12] studied the use of Multidisciplinary Design Optimization (MDO) to achieve a quiet small propeller. Their method was then applied in the experimental and analytical study of two propellers configured for small UAVs[13], one conventional design and another one with a narrow tip chord, optimized for acoustics. The results show an improvement in the noise level of the optimized propeller compared to the conventional one especially in its tonal characteristics. However, their numerical analysis for tone noise using Farassat and Succi's[14] method underpredicted sound levels.

It is apparent that better understanding of acoustic phenomena at these small scales is necessary for achieving reliable noise prediction in drone applications, not only for a single rotor but also for the contribution of multiple rotors. We are particularly interested in the complexity of the flow field of a quadcopter and the associated acoustic sources of such system, namely the interaction of the rotor wake flow with the underlying support structure as well as the interaction of a given rotor with adjacent rotors.

This paper presents the preliminary aeroacoustic study of a quadcopter system using a readily available DJI Phantom II drone as a test model. This experimental study focuses on the performance and noise created by four different commercially available rotor blade designs to capture broad characteristics of quadcopter noise and the effects of operating a varying number of rotors at a given time.

II. Apparatus and Instrumentation

Thrust and acoustic measurements for the quadcopter were performed simultaneously in the Virginia Tech anechoic chamber, designed by Eckel Industries. The chamber is fully anechoic providing a low frequency cut-off of 100Hz and has interior dimensions of 5.4 m x 4.1 m x 2.4 m.

A. Test model

The DJI Phantom II quadcopter was selected as the study platform without any modifications to the fuselage, power or propulsion system. The decision to use the DJI Phantom II as a test model were based on its popularity and accessibility. The quadcopter weighs approximately 1.04kg without propellers, resulting in 10.23 N of thrust required for takeoff. To allow for precise rotor control inputs, a Digi Xbee Pro RF module was installed to the quadcopter circuit to establish a line of communication with a data acquisition computer. Control inputs were sent in the form of pulse width modulation through a LabView-based program. All four rotors can be controlled independently for operation of 1, 2, 3 or 4 propellers as desired. Figure 1 shows a setup of the DJI Phantom II quadcopter mounted in the anechoic chamber. Detailed photos of the quadcopter mounting are given in Figure 2.

The current study focuses on the aeroacoustic performance of 4 different rotor blade sets available in the market for the DJI Phantom II (Figure 2.c). These rotor sets include, first, the original DJI propeller, model 9450, with a 239mm diameter. The second set was an aftermarket version of the DJI propeller, model 9443 and had the same diameter. The model 9450 design was developed (by DJI) to improve thrust performance over the model 9443. For this study, the OEM version was not available and the aftermarket version was therefore chosen. These first two propellers are made of plastic whereas the other two are constructed from carbon fiber. Despite looking much different than the authentic model 9443, the third propeller is a black carbon fiber aftermarket prop modelled after the DJI 9443 version. The last propeller, seen in white in Figure 2.c, is a completely difference design by T-motor, measuring only 229 mm in diameter. It is also has the smallest averaged chord. The four propellers will be referred to in this report as Original, Aftermarket, Black Carbon and White Carbon respectively.

The majority of the tests were conducted by having all 4 rotors of the quadcopter operating at the same approximate rotational speed to examine multiple rotor interaction. Based on the DJI Phantom fuselage design, it is possible for two propeller tips to pass in close proximity to each other (as seen in Figure 3.a). In addition, the tips periodically pass very close to the rotor arms (Figure 3.b). Only the Original and the White Carbon propeller were tested at conditions with a reduced number of rotors in operation. Both were investigated for their aeroacoustic performance when dual clockwise rotors were in motion while the other two counter-clockwise rotors stayed

motionless as diagrammatically displayed in Figure 4.b. Only the Original prop was tested for a single rotor performance using the clockwise rotor closest to the microphone (see Figure 4.b).

Initial measurements of the propeller rotational speed by a stroboscope showed that there were slight variations in RPM across all 4 rotors for a given control pulse width setting. Therefore, the shaft rate and blade passage frequency are computed from acoustic spectra.

B. Thrust measurements

To measure static thrust, the quadcopter was attached to an LC101-25 Omega S-beam load cell through aluminum adapters as displayed in Figure 2.a. Another set of aluminum adapters connected it to a floor anchor through a single aluminum vertical rod 31.75-mm in diameter, thus placing the bottom of the quadcopter 0.77m off the chamber grate floor. Three steel cables tightened the rod to other floor anchors in order to eliminate vibrations. The axis of the load cell was aligned with the center of the quadcopter to balance its off-axis loads. The load cell was statically calibrated against a series of known weights before and after the test, yielding repeatable results. The maximum range for the LC101-25 load cell is ± 116.15 N with an uncertainty of ± 0.35 N. The thrust signals from the load cell were averaged and tare values were subtracted to produce the net static thrust of the quadcopter.

C. Microphone measurements

A single ½" Bruel & Kjaer 4190 microphone was used to record the noise produced by the quadcopter. It was placed 0.77m below the top of the quadcopter fuselage and 1.30m to the side (in the direction parallel and in-line with the battery compartment as seen in Figure 4.a). The distance from the drone center to the microphone is 1.51m, equivalent to 6.3 times the blade diameter. The directivity angle is close to 50 degrees to the propeller rotational axis. Signals from the microphone and load cell were digitized and recorded using 24-bit Bruel & Kjaer LAN XI modules and Pulse 14 software. Data were sampled at 65,536 Hz for 32 seconds. Acoustic spectra presented in this report were averaged over 511 records of 8,192 samples each with Hanning windowing and 50% overlap between records. The microphone uncertainty is ± 1dB up to 20 kHz.

III. Results and Discussion

A. Aerodynamic Performance

Aerodynamic performance of different rotor sets can be observed in Figure 5 where the net thrust obtained from the load cell is plotted against the averaged rotor RPM. The averaged rotor RPM was acquired by extracting the shaft rotation rate from the noise frequency spectrum (this was done as the 4 rotors turned at slightly different RPMs). Plotted in Figure 5 are thrust results from the Original, Aftermarket, White Carbon and Black Carbon propeller with all four rotors in operation. Also displayed in the figure is the takeoff thrust required by the quadcopter as a horizontal dash line at 10.32N. For the same RPM, the Original 9450 propeller can be seen to clearly produce the highest thrust. The difference between the thrust of the Original 9450 propeller and the second highest thrust propeller (the Aftermarket 9443 model) varies from 25 to 42 percent for the same RPM setting, agreeing with the manufacturer's claim of improved performance in the 9450 propeller over its preceding design. The two carbon fiber propeller, despite being completely different in blade pitch and chord distributions, have almost identical thrust performance across the entire range of rotational speed in this study, while both being significantly lower (40 to 50%) than the Original 9450. This poor performance for two radically different propellers suggests they may both experience some form of blade stall. A vast variation in thrust performance of these 4 rotor configurations with nearly identical diameter indicates sensitivity of blade geometries to aerodynamics of small-scale rotors.

When tested with just a single or dual rotor spinning (Figure 6), the net thrust varies with the RPM similar to when all 4 rotors are spinning. A single rotor of the Original 9450 does not produce enough thrust to lift the quadcopter off the ground even at the maximum RPM. Figure 7 shows a ratio of multi-rotor to single-rotor thrust of the Original propeller for both quad and dual rotor configuration. Interestingly, the thrust produced by 4 rotors and 2 rotors is not 4 and 2 times the single rotor thrust, these results confirms that rotor interaction can reduce the propeller aerodynamic performance. On average, the thrust is reduced 5.8% when going from 1 to 2 rotors and 7.3% for 4 rotors in comparison to scaled single rotor performance.

B. Characteristics of Quadcopter Acoustics

The signal-to-noise ratio of acoustic measurements in the anechoic chamber was at least 12 dB for frequencies greater than 100 Hz. Figure 8 shows narrowband power spectra density of the background noise compared to that of the Original propeller operating at 3840 RPM (nominally the RPM required for takeoff of the Original propeller)

and the unloaded motor (without any propeller) at a similar rotational speed of 3360 RPM. Both measurements feature all 4 rotors in operation. Examining the unloaded motor spectrum indicates that the motors noise contributes to the overall noise signature of the drone in the mid frequency range (600-6000 Hz) increasing at least 22 dB on par with the total system noise in this range. The unloaded motor spectrum also shows several tones across the entire frequency spectrum with amplitude as high as 34 dB at 832 and 2240 Hz. Around these frequencies, the motors can be seen to be the main contributor to the overall noise levels. At higher frequencies, above 6000 Hz, the overall sound levels of the 4 loaded rotors is well above the motor signature (itself at least 10dB above the background) suggesting that the noise source in this range is not due to the motor, but is presumably aerodynamically generated sound.

The characteristics of the quadcopter noise can also be observed in Figure 8 from the Original propeller tested at 3840RPM. Tonal and broadband noise dominate the quadcopter spectrum at the shaft rate (64 Hz) and the blade passing frequency, (128 Hz), as well as their harmonics. Even though the shaft rate for this test condition is lower than the chamber cutoff frequency, it is undeniably distinctive when compared to the low background noise and as high as 19 dB above the broadband floor. The humps at the blade passing frequency, BPF, are much louder than at the shaft rate peaking at 45dB and maintaining this power level up to the 4th harmonic. The subsequent harmonics still sustain high amplitude (32 to 38dB) to a much higher frequency until the motor noise and underlying broadband features begin to dominate. The domination of the BPF and the smaller shaft rate noise is similar to the typical acoustic spectrum of axial flow machines proposed by Wright[9]. Around the mid frequency range, some harmonics of the BPF have amplitudes nearly as high as the fundamental frequency (around 2800 Hz), which can be seen to coincide with tone noise from the motors.

It is also interesting to investigate the broadband level of the Original propeller spectrum in Figure 8. This spectrum plot shows an increase in broadband noise to 20dB and higher after 600 Hz, nearly 10dB above the broadband level at lower frequency range. The broadband noise rolls off after 6000 Hz. This broadband hump may come from rotor self-noise. A similar broadband hump was measured in Ref 10 for a propeller of comparable size and rotational speed and was shown to be caused by a thickening of the trailing edge boundary layer induced by a separation bubble. The hump peak also coincides with the maximum of the motor noise in the mid frequency range. It should be noted that this static test of the quadcopter was performed in a closed anechoic chamber. As a result, the rotor wake may recirculate in the chamber and result in turbulence self-ingestion back to the rotors. It is therefore possible that some of the tonal and broadband components seen in the spectrum may be in part due to this phenomenon.

The impact of the different propellers on the drone noise spectrum is presented in Figure 9. This figure compares acoustic spectra of 4 rotor sets running at 4000 RPM. Since they were tested at slightly different RPM, the frequency of tone noise at the shaft rate and BPF can be seen to be slightly misaligned. The noise characteristics of the other three non-OEM propellers are almost identical to the Original propeller at low frequency with tone and broadband magnitude varying due to the difference in blade loading. Motor noise can again be seen to be the main contributor to those spectra at mid frequencies. At high frequencies, however, there are deviations in the broadband roll-off between the different propellers. For the Black Carbon propeller (teal curve), there is a high tone noise with broadband content at 15 kHz which may indicate laminar boundary layer vortex shedding noise. The broadband hump of the Black Carbon also rolls off much later (and faster) than the other propellers. There are no clear indication of vortex shedding noise in the other spectra. Nevertheless, with their operating conditions close to fully laminar over the entire blade sections and rotor span, laminar boundary layer tones may spread out over a wide frequency range giving a broadband-like spectrum depending on blade relative velocity[15]. Interestingly, while the White and Black Carbon propellers produced almost identical thrust, their noise spectra clearly diverge at frequencies above 6000Hz, with the White carbon prop consistently 5dB lower. It is also important to note that at these high frequencies, the Black carbon noise spectrum displays similar broadband levels as both the Original and Aftermarket configurations even though the thrust it produced is 40 to 50% lower, highlighting its acoustic inefficiency.

At a higher rotational speed of 6000 RPM (Figure 10), the noise spectra are similar to the results at lower RPM shown in Figure 9. The vortex shedding tone at high frequency of the Black Carbon propeller has disappeared and is replaced with a lower broadband-like hump. Thus, it is likely that the increased blade angle of attack at higher RPM has disrupted the vortex shedding mechanism which has been shown to occur at low angle of attacks[16]. It is also important to note that the deviation between the White and Black carbon propellers starts at a higher frequency (10 kHz compared to 6 kHz at 4000RPM).

To assess the noise characteristics of the different rotor sets independently of the blade loading, spectra of similar thrust settings for each propeller are plotted together in Figure 11.a as a function of the BPF harmonics. Figures 11.b through c present direct comparison of each of the 3 non-OEM propellers against the Original baseline.

Apart from the Black Carbon propeller tested at 16.8N, the other rotor sets have nearly identical net thrust at approximately 17.5N. Since each rotor runs at different RPM, to achieve the same thrust setting, the spectra were presented as harmonics of the blade passing frequency for a better comparison. Figure 11.a displays the spectra content up to the 20th harmonic which denotes the similarity of the tone magnitude at low frequency for all four propellers when compared at the same thrust setting. The non-uniformity in the rotational speed of multiple rotors can also be seen at higher harmonics where a number of secondary peaks appear. At higher frequency (Figures 11.b , c and d), the White Carbon propeller continues to creates a distinct tone up to 55th harmonics of the BPF (or approximately 12kHz), having higher amplitude than the tone created by the Aftermarket and the Black Carbon propellers. The Original propeller's tone noise has disappeared (Figure 11.b) under the broadband noise from the 35th harmonics (or 6 kHz) since it operates at the lowest RPM. At high frequency, the broadband noise level of the White Carbon is lowest. The results denote that propeller configurations have a distinct influence over broadband content.

The overall sound pressure level (OASPL) is computed by integrating the noise spectra from 100 Hz – 20 kHz and presented in A-weighed dB in Figure 12 at various thrust setting with all 4 rotors spinning. At takeoff condition, the OASPL is undiscernible between all rotor sets at approximately 70dBA, already higher than the level of a normal conversation of 60dBA at 1 meter away. At higher thrust settings, the Original and Aftermarket propeller, having similar OASPL, yields noise levels 1-2 dBA lower than the other 2 rotors. The White Carbon propeller generates the loudest sound for the same thrust setting due to its higher tone amplitude near the mid frequency range shown in Figure 11. At the maximum thrust setting measure in this study, every propeller reaches an OASPL of about 80 dBA. In term of OASPL, this places the noise produced by the DJI Phantom II quadcopter on par with the noise produced by a freight train passing 15m away (a level that would most likely trigger annoyance in populated areas subjected to high drone traffic).

C. Interaction of multiple rotors

To evaluate the effect of rotor interaction, the power spectral density of the Original and White Carbon rotors at 6000 RPM are presented in Figure 13 (note that the associated thrust values are presented in the legend). At 6000 RPM, the spectra in Figure 13.a reveal that the acoustic spectra of a single, dual and quad Original rotor are all similar in their characteristics with variations occurring primarily in the amplitude of the spectra. Operating single or dual rotors results in the same extensive tonal component in the spectra akin to that found with 4 rotors spinning. The broadband hump near mid frequency is also present in the single and dual rotor operation. However, there is a more substantial increase in the broadband noise level from the 2 rotor case to the 4 rotor case (Figure 13.c) than what is seen when going from 1 rotor to 2. It is interesting to see that tones at the BPF and its harmonics for 1 and 2 rotors are identical over the entire frequency range. When increasing to 4 rotors, the amplitude of these tones increases by 3-8dB (Figure 13.b and c) at almost all frequencies. At the same time, the increase in the broadband levels going from 1 to 2 rotors is about 3dB, but it reaches 6-8dB going from 2 to 4 rotors. The increment of noise from 2 to 4-rotor operation is more than double the sound pressure. This non-linear increase suggests that interactions between rotors are likely a contributing factor (with the 4-rotor configuration experiencing interactions between 4 pairs of counter-rotating rotors). Two-blade operation has less rotor-to-rotor interaction due to the increased spacing between blade sets.

On the other hand, the White carbon propeller (Figure 13.d) does not show such scaling effects in the tone amplitude at lower frequencies (<1 kHz) but there is significant change in the broadband levels. It is possible that some of the observed differences around the BPF and its harmonics may be due to the asynchronized sampling scheme which disregards the rotational rate of the blade sets. This could artificially broaden the measured response around the BPF and its harmonics, but it is interesting to compare differences in the broadband for the two data sets at frequencies above 6 kHz. The smaller rotor diameter of the White carbon blade may reduce the rotor-to-rotor interaction due to the larger distance between blade tips of two consecutive rotors. Switching from 2 to 4 propeller operation results in a 3-5dB increase, which is noticeably less than for the Original blades. Also, the spectrum of the White Carbon rotor with 2 rotor operations also show a sign of vortex shedding near 15 kHz that disappears when 4 rotors operate.

IV. Conclusion

An experimental study of quadcopter aeroacoustic performance was carried out in the Virginia Tech anechoic chamber using a single microphone and an S-beam load cell. Noise and thrust produced by the DJI Phantom II drone at static conditions were investigated for 4 different commercially available propeller configurations, an original DJI 9450 model (Original), an aftermarket DJI 9443 model (Aftermarket), another aftermarket 9443 replica (Black

Carbon) and a T-motor designed propeller (White Carbon). The drone was set to operate in single, double and quad rotor modes between 1500 and 8000 RPM to evaluate effects of multi-rotor interactions. The following conclusions was drawn.

- Thrust produced by small-scale rotors is sensitive to the blade geometry and rotor configuration.
- The interaction between multiple rotors can decrease aerodynamic performance. In the case of the Original 9450 propeller, thrust reduced by 5.8% for 2 rotor operation and 7.3% for the 4 rotor operation in comparison to scaled single rotor performance.
- The acoustic spectra of the quadcopter is dominated by high and sustained tone noise at the blade passing frequency and shaft rate and their harmonics up to the mid frequency range (around 6 kHz).
- Broadband noise in the spectra become dominant in the mid and high frequency ranges indicate that rotor self-noise could be significant part of the system noise.
- There are signs of laminar boundary layer vortex shedding noise at some rotational speeds for the White and Black Carbon propeller.
- Motor noise helps contribute to the level of tone and broadband noise in the mid frequency range.
- Variations in the acoustic spectra of different rotor sets at the same thrust are significant around the mid and high frequencies at which the broadband component dominate.
- Besides some variations in the broadband noise at mid and high frequency, the overall sound pressure level in dBA is nearly identical at the same thrust setting for different rotor sets with a maximum of 2dB difference for all rotor sets.
- Compared to 1 or 2-rotor operation, the 4-rotor interaction produces a significant increment in broadband noise.

Acknowledgments

The authors would like to thank Aurora Flight Sciences and Panoptes Systems for the use of the quadcopter.

References

[1]L. Dorr, Jr. and A. Duquette, "Press Release – U.S. Transportation Secretary Foxx Announces FAA Exemptions for Commercial UAS Movie and TV Production". *[Online]*. Available: http://www.faa.gov/news/press_releases/news_story.cfm?cid=TW251&newsId=17194, 25 September 2014.

[2]A. Lucieer, D. Turner, D. H. King and S. A. Robinson, "Using an Unmanned Aerial Vehicle (UAV) to Capture Micro-topography of Antarctic Moss Beds," *International Journal of Applied Earth Observation and Geoinformation*, pp. 53-62, 2014.

[3]M. E. Goebel, W. L. Perryman, J. T. Hinke, D. J. Krause, N. A. Hann, S. Gardner and D. J. LeRoi, "A Small Unmanned Aerial System for Estimating Abundance and Size of Antarctic Predators," *Polar Biology*, vol. 38, no. 5, pp. 619-630, May 2015.

[4]M. A. Ditmer, J. B. Vincent, L. K. Werden, J. C. Tanner, T. G. Laske, P. A. Laizzo, D. L. Garshelis and J. R. Fieberg, "Bears Show a Physiological but Limited Behavioral Response to Unmanded Aerial Vehicles," *Current Biology*, pp. 2278-2283, 2015.

[5]C. Dillow, "Get Ready for 'Drone Nation'". *[Online]*. Available: http://fortune.com/2014/10/08/drone-nation-air-droid/, October 2014 [Accessed 26 April 2016].

[6]J. B. Brandt and M. S. Selig, "Propeller Performance Data at Low Reynolds Numbers," in *49th AIAA Aerospace Sciences Meeting*, Orlando, FL, 2011.

[7]M. P. Merchant and L. S. Miller, "Propeller Performance Measurement for Low Reynolds Number UAV Applications," in *44th AIAA Aerospace Sciences Meeting and Exhibit*, Reno, NV, 2006.

[8]T. B. Carroll, I.-R. George, G. Bramesfeld and K. Raahemifar, "Design Optimization of Small Rotors in Quad-rotor Configuration," in *54th AIAA Aerospace Sciences Meeting*, San Diego, CA, 2016.

[9]S. E. Wright, "The Acoustic Spectrum of Axial Flow Machines," *Journal of Sound and Vibration*, vol. 45, no. 2, pp. 165-223, 1976.

[10]A. Leslie, K. C. Wong and D. Auld, "Broadband Noise Reduction on a Mini-UAV Propeller," in *14th AIAA/CEAS Aeroacoustics Conference*, Vancouver, British Columbia, May 2008.

[11] A. Leslie, K. C. Wong and D. Auld, "Experimental Analysis of the Radiated Noise from a Small Propeller," in *20th International Congress on Acoustics ICA 2010*, Sydney, Australia, August 2010.

[12]O. Gur and A. Rosen, "Design of a Quiet Propeller for an Electric Mini Unmanned Air Vehicle," *Journal of Propulsion and Power*, vol. 25, no. 3, pp. 717-728, 2009.

[13]G. Sinibaldi and L. Marino, "Experimental Analysis on the Noise of Propellers for Small UAV," *Applied Acoustics*, vol. 74, no. 1, pp. 79-88, 2013.

[14] F. Farassat and G.P. Succi, "A Review of Propeller Discrete Frequency Noise Prediction Technology with Emphasis on two Current Methods for Time Domain Calculations", *Journal of Sound and Vibration*, vol. 71, no. 3, pp. 399–419, 1980.

[15]R. W. Paterson and R. K. Amiet, "Noise of a Model Helicopter Rotor Due to Ingestion of Isotropic Turbulence," *Journal of Sound and Vibration*, vol. 85, no. 4, pp. 551-577, 1982.

[16] A. S. Hersh, P. T. Soderman, and R. E. Hayden, "Investigation of Acoustic Effects of Leading-Edge Serrations on Airfoils", *Journal of Aircraft*, vol. 11, no. 4, pp. 197-202, 1974.

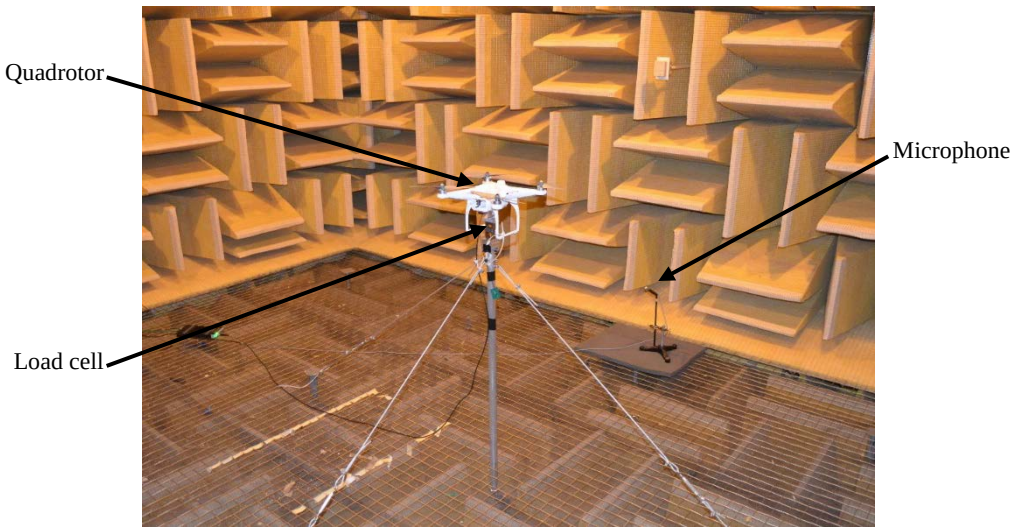

Figure 1. Test setup in the anechoic chamber for thrust and acoustic measurements

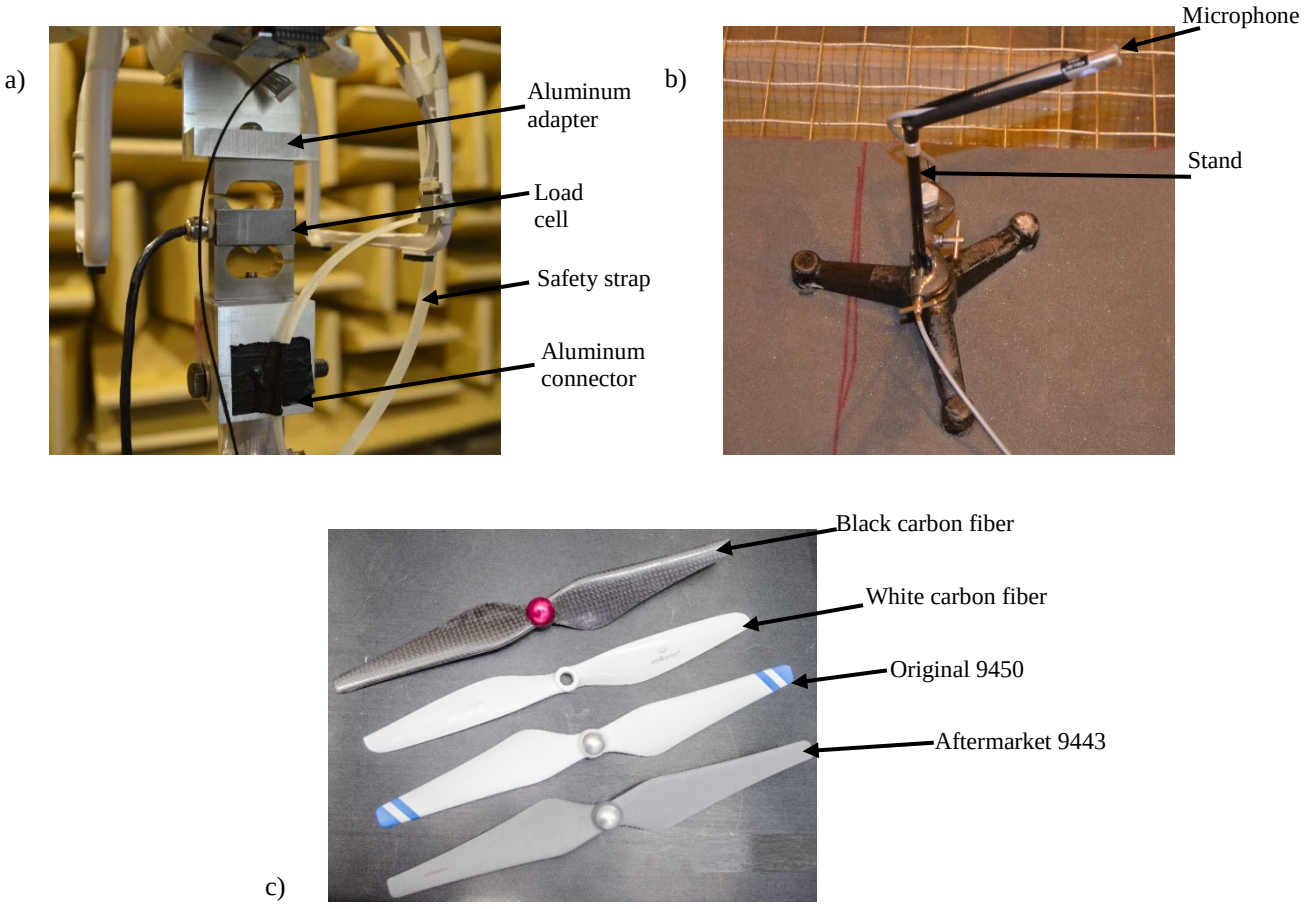

Figure 2. a) LC101-25 Omega S-beam load cell connected to the bottom of the quadcopter. b) ½ in Bruel & Kjaer 4190 microphone on a floor stand. c) Four rotor props selected for this test.

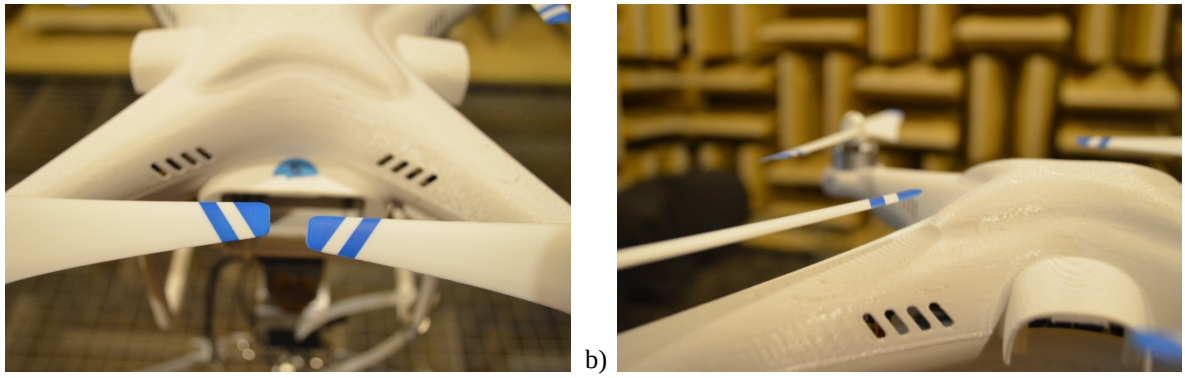

Figure 3. Close observation of proximity between a) two rotor tips and b) a rotor tip and the quadcopter arm.

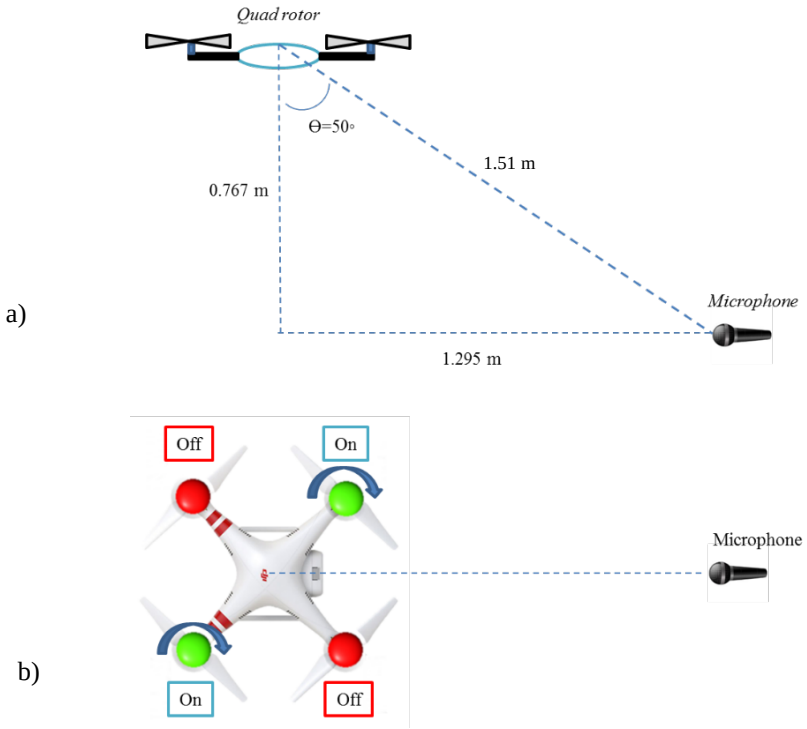

Figure 4. a) Diagram of microphone location (side view) and b) microphone setup with respect to rotor rotational direction (top view).

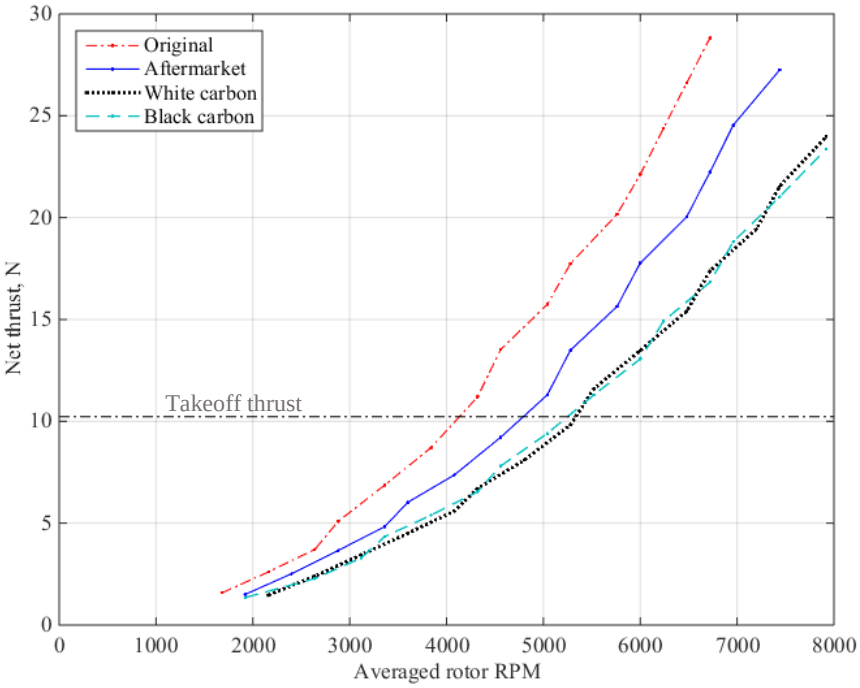

Figure 5. Static thrust of four propeller sets

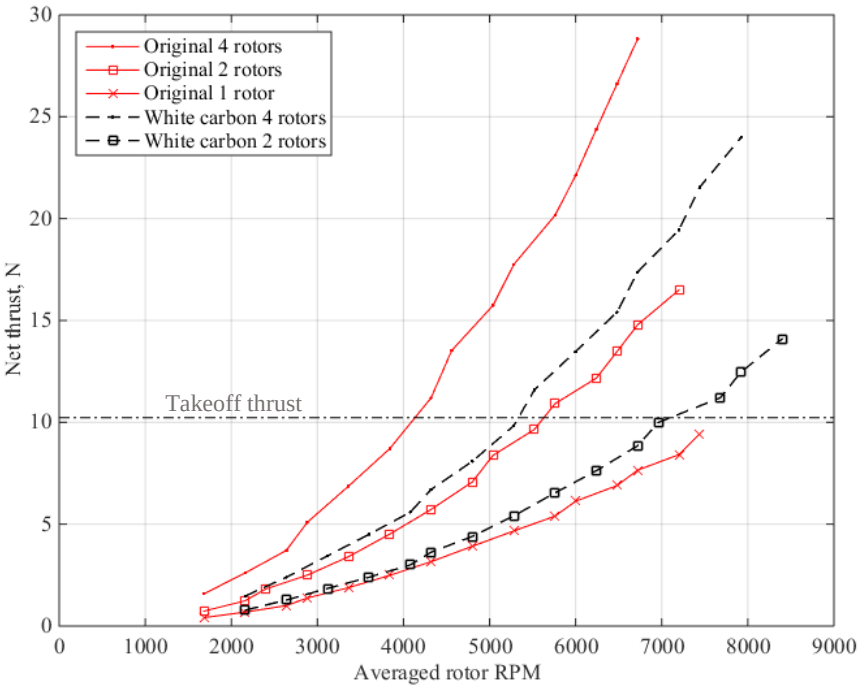

Figure 6. Static thrust of single and 2 rotor operation compares to 4 rotor operation for the Original 9450 and White Carbon propeller set.

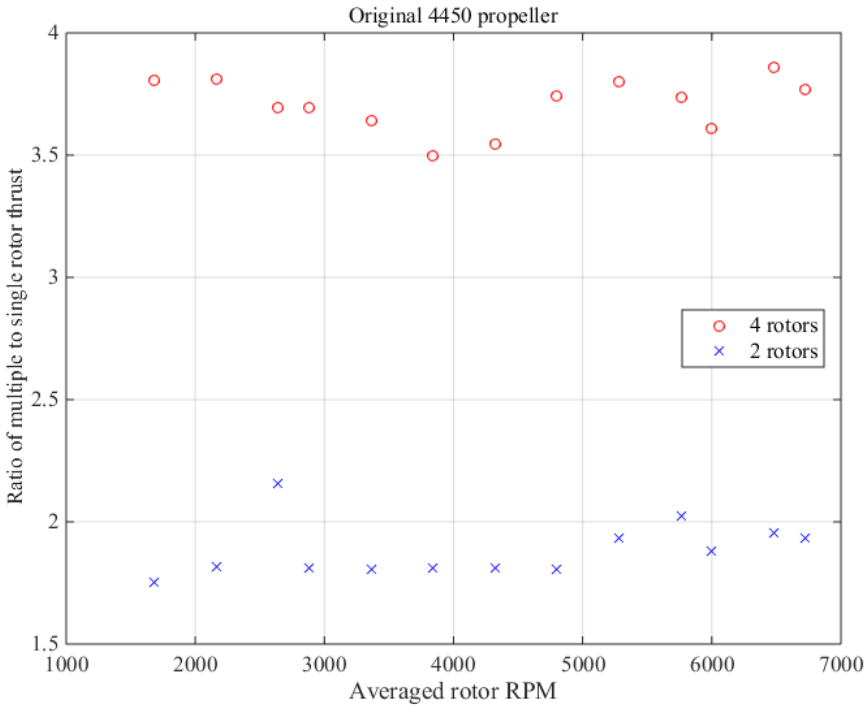

Figure 7. Ratio of thrust produced by 2 and 4 rotors to that of a single rotor for the Original 9450 propeller.

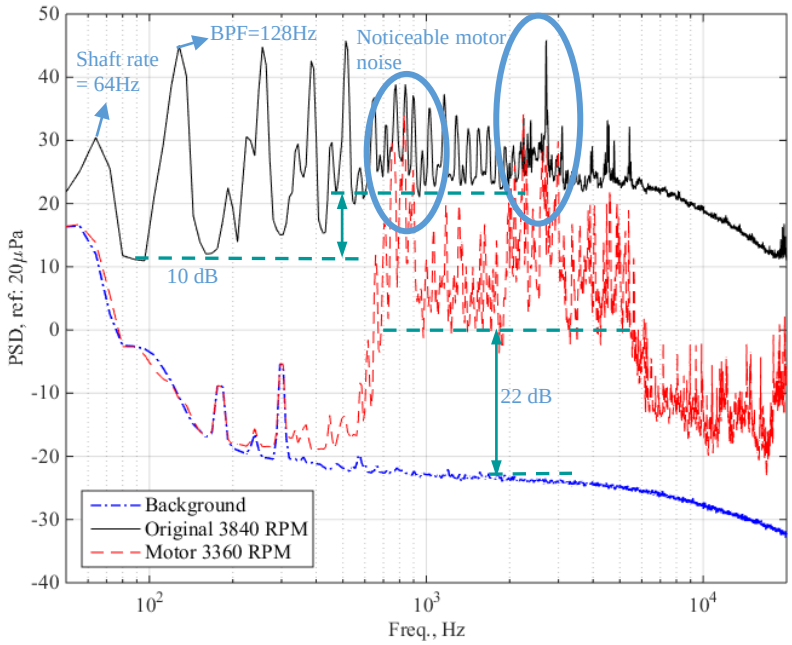

Figure 8. Power spectral density of the Original 9450 propeller compares to that of the unloaded motor running at nominal motor rotational speed of 4000 rpm and background noise in the anechoic chamber.

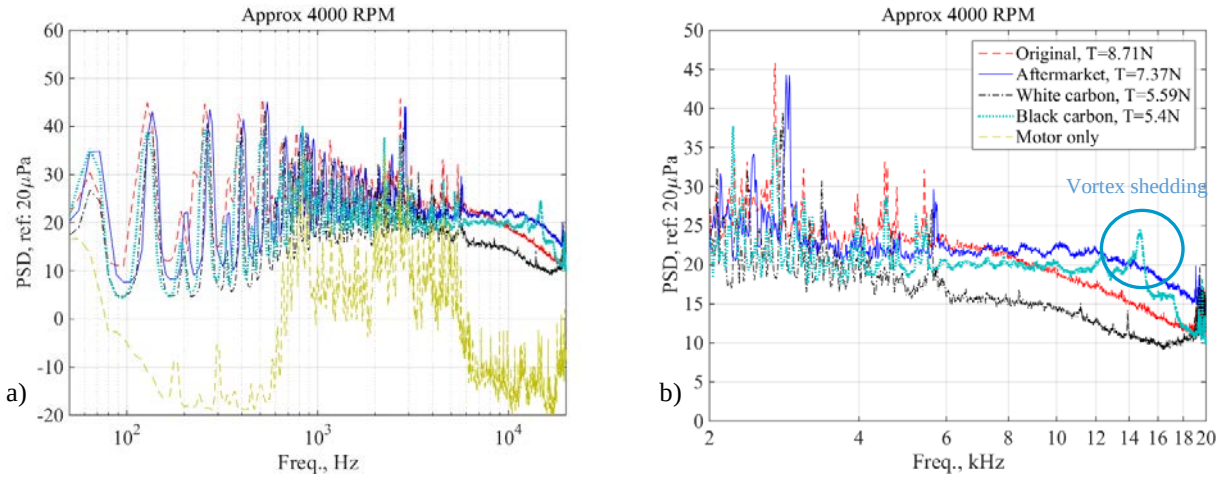

Figure 9. Power spectral density of four propeller configurations running at nominal motor rotational speed of 4000 RPM. a) 50 Hz – 20 kHz with unloaded motor noise and b) 2 kHz – 20 kHz with a legend to be used in a) as well.

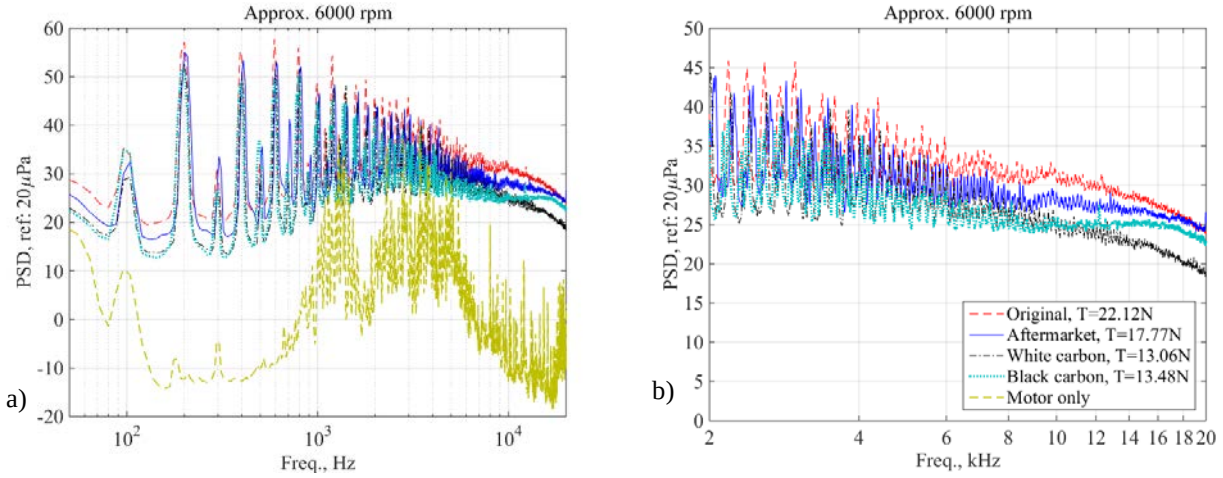

Figure 10. Power spectral density of four propeller configurations running at nominal motor rotational speed of 6000 RPM. a) 50 Hz – 20 kHz with unloaded motor noise and b) 2 kHz – 20 kHz with a legend to be used in a) as well.

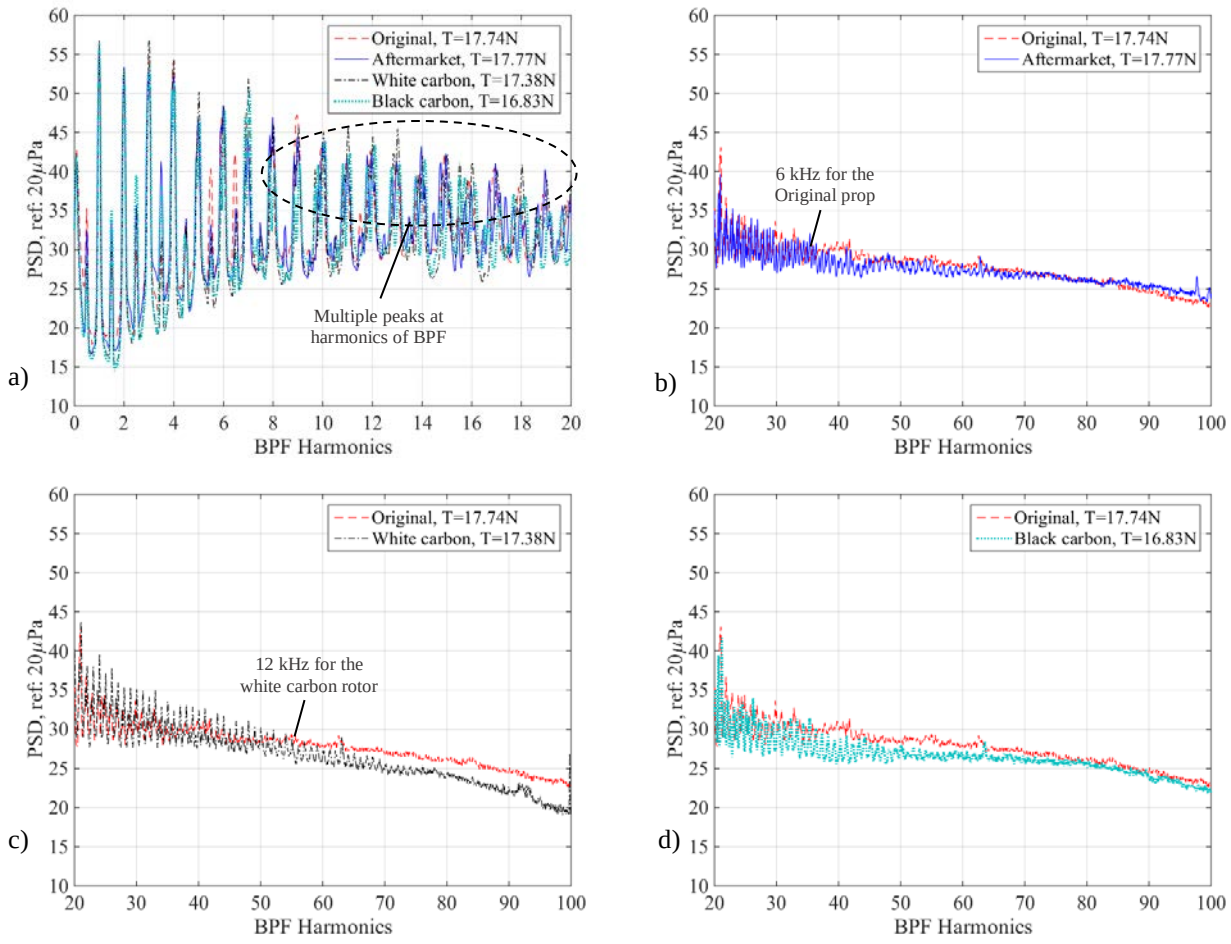

Figure 11. Power spectral density of four propeller configurations running at equivalent thrust setting of 17 N. a) Spectra of 4 propeller configurations up to the 20th harmonic. b) Spectra of the Original and Aftermarket from 20th-100th harmonic. c) Spectra of the Original and White Carbon from 20th-100th harmonic. d) Spectra of the Original and Black Carbon from 20th-100th harmonic.

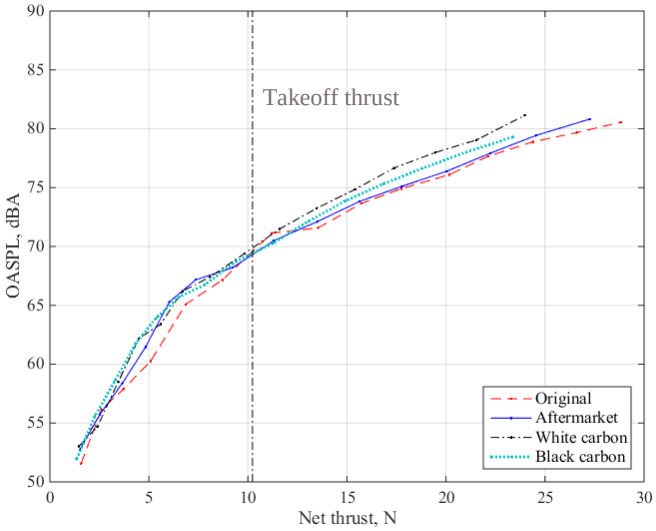

Figure 12. Overall sound power level of four propeller configurations

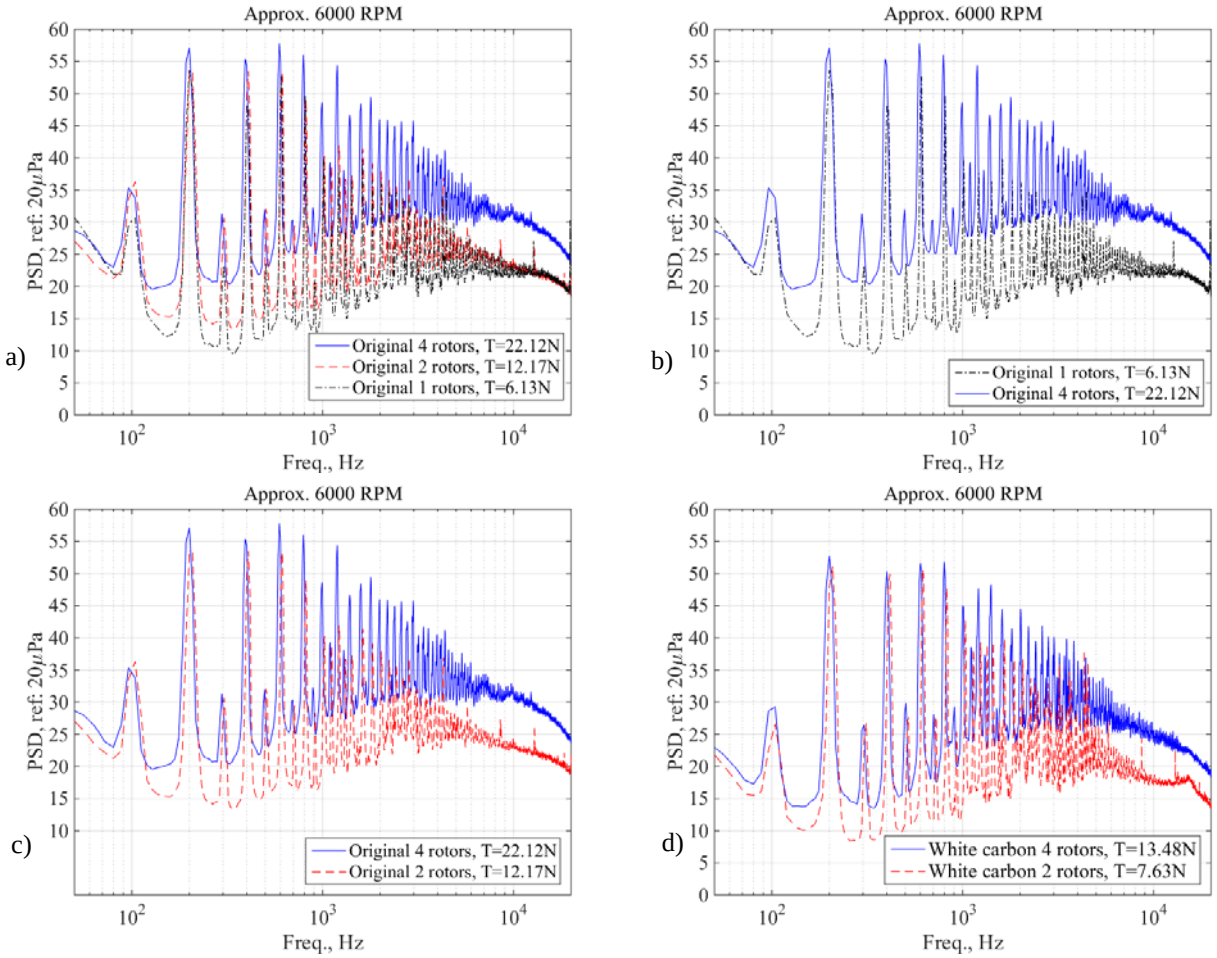

Figure 13. Power spectral density of the Original 9450 and White Carbon propeller operate with 1, 2 and 4 rotors at the nominal rotational speed of 6000 RPM. a), b) and c) Spectra of the Original propeller. d) White Carbon.